Chemical Science

ROYAL SOCIETY OF CHEMISTRY

EDGE ARTICLE

View Article Online
View Journal | View Issue

Cite this: *Chem. Sci.*, 2021, **12**, 6747

All publication charges for this article have been paid for by the Royal Society of Chemistry

Catalyst design in C–H activation: a case study in the use of binding free energies to rationalise intramolecular directing group selectivity in iridium catalysis†

William J. Kerr, * Gary J. Knox, Marc Reid * and Tell Tuttle

Remote directing groups in a bifunctional molecule do not always behave independently of one another in C–H activation chemistries. A combined DFT and experimental mechanistic study to provide enhanced Ir catalysts for chemoselective C–H deuteration of bifunctional aryl primary sulfonamides is described. This provides a pharmaceutically-relevant and limiting case study in using binding energies to predict intramolecular directing group chemoselectivity. Rational catalyst design, guided solely by qualitative substrate–catalyst binding free energy predictions, enabled intramolecular discrimination between competing *ortho*-directing groups in C–H activation and delivered improved catalysts for sulfonamide-selective C–H deuteration. As a result, chemoselective binding of the primary sulfonamide moiety was achieved in the face of an intrinsically more powerful pyrazole directing group present in the same molecule. Detailed DFT calculations and mechanistic experiments revealed a breakdown in the applied binding free energy model, illustrating the important interconnectivity of ligand design, substrate geometry, directing group cooperativity, and solvation in supporting DFT calculations. This work has important implications around attempts to predict intramolecular C–H activation directing group chemoselectivity using simplified monofunctional fragment molecules. More generally, these studies provide insights for catalyst design methods in late-stage C–H functionalisation.

Received 15th March 2021
Accepted 1st April 2021

DOI: 10.1039/d1sc01509e

rsc.li/chemical-science

Introduction

The evolving synergy between experimental and computational chemistry is central to the study of organometallic reactions, and now permeates most aspects of catalysis, mechanistic studies, ligand design, and chemoinformatics.[1–7] Among the areas of organometallic chemistry capitalising on this contemporary investigative approach, C–H activation is notably prevalent.[8,9] However, while the use of theory to rationalise and analyse experimental results is increasingly common, application of these methods to the prediction and design of new catalysts remains less so.

An understanding of site selectivity is vital for the implementation of late-stage C–H functionalisation methods in organic synthesis.[10–12] Yet, relative to the number of synthetic developments, fundamental studies on site selectivity in complex molecules are rare.[13–21] In our laboratories,[18,22–25] we have explored iridium-catalysed C–H activation and hydrogen isotope exchange (HIE) protocols[26–31] for application in pharmaceutically-relevant labelling studies. Importantly, such studies also serve as an insightful proxy for determining site selectivity in other C–H functionalisation processes.[32–38] In relation to this, we recently reported a rare example of *ortho*-C–H activation and deuteration of aryl primary (1°) sulfonamides.[24] In the course of these studies, when labelling bifunctional sulfa drug **1**→**3**, sterically-distinct precatalysts **2a** and **2b** labelled **1** with dramatically different selectivities, with neutral NHC/Cl catalyst **2a** directing labelling *ortho* to the sulfonamide, and cationic NHC/phosphine catalyst **2b**

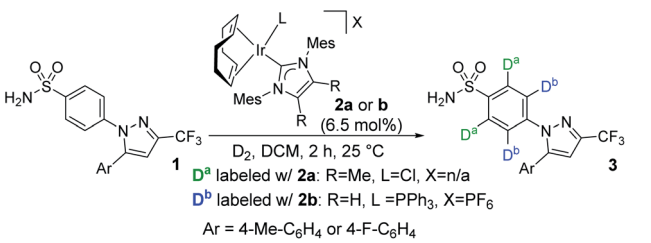

Scheme 1 Catalyst-enabled switching of directing group chemoselectivity in the deuterium labelling of sulfa drugs.

Department of Pure & Applied Chemistry, WestCHEM, University of Strathclyde, Glasgow G1 1XL, Scotland, UK. E-mail: w.kerr@strath.ac.uk; marc.reid.100@strath.ac.uk

† Electronic supplementary information (ESI) available. See DOI: 10.1039/d1sc01509e

leading to deuterium incorporation *ortho* to the pyrazole unit (Scheme 1).

Mechanistic analysis led to an enhanced understanding of this intramolecular *ortho*-directing group (DG) selectivity. Specifically, it was found that, in the face of energetically similar C–H activation barriers proceeding *via* sigma-complex assisted metathesis, the substrate–catalyst binding event (through either sulfonamide or pyrazole *ortho*-directing groups) was found to be the product-determining step.[24] Furthermore, the choice of catalyst **2a** or **2b** was sufficient to completely alter the observed labelling chemoselectivity from one directing group to the other. Crucially, directing group selectivity in these bifunctional molecules could not be predicted on the basis of competition experiments with the individual sulfonamide and pyrazole fragments.[24] We have therefore undertaken practical and theoretical studies to further develop the qualitative (semi-quantitative) understanding of intramolecular directing group selectivity in the context of rational catalyst design for *ortho*-C–H activation with aryl 1° sulfonamides (Scheme 2).

Computational details

Consistent with previous studies on related systems,[24,25] the vast majority of calculations employed the M06 density functional in conjunction with the 6-31G* basis set for main group non-metal atoms and the Stuttgart RSC effective core potential along with the associated basis set for Ir. This level of theory – with and without solvation – has been employed successfully by our group,[24,25,39] and others,[13] in previous reports for related systems, serving as the minimum viable level of theory to produce qualitative direction for experimental catalyst design strategies. Additional calculations employing the Polarization Continuum Model[40] for DCM solvation have been included and stated explicitly where it has been relevant to highlight the limitations of the predictive binding free energy model under investigation. As detailed in the Results section, our original aim was not to provide a high-level quantitative model, but rather a simple qualitative predictor of labelling selectivity *via* examination of differences in directing group binding free energy alone. This approach is based on findings from our previous publication, wherein combined binding and transition state calculations showed that binding free energy differences alone could be semi-quantitative predictors of directing group chemoselectivity in the presence of various catalysts.[24] While the energy of the transition state will have an effect on the rate and efficacy of a reaction, the aforementioned previous investigations have shown that the transition state energy, in the Ir C–H activation catalyst types under consideration, is not strongly affected by the directing groups. Therefore, the relative energy difference between the initial bound states of each available directing group in the substrate creates an effective higher activation energy for the weaker bound complex, which invites the assumption that the difference in binding free energy is product determining. Free energy differences for $\Delta(\Delta G_{bind})$ displayed herein are as a result of manually exploring reasonable conformational substrate–catalyst binding space and calculating Boltzmann distributions where appropriate. All calculated conformations were found to exist within approximately 10–15 kcal mol^{-1} of the global minimum. The Boys–Bernardi counterpoise scheme was employed for the exploration of electronic binding energies deconstructed into favourable and distorting interactions between catalyst and substrate fragments. All counterpoise calculations were conducted using geometries previously optimised in either gas phase or DCM, as appropriate. Importantly, counterpoise calculations themselves possess no information on free energy, and contain only electronic energy contributions. Full details of and references to the theoretical methods are contained within the ESI†.

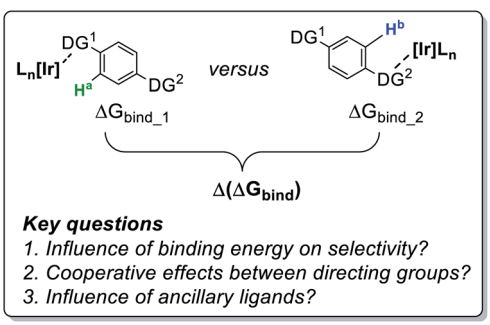

Scheme 2 Key mechanistic questions for the current investigation.

Results

Understanding bifunctional substrate properties

Before commencing our investigations and as delineated in the Computational details section, it was hypothesised that the simple thermodynamic parameter $\Delta(\Delta G_{bind})$ (Scheme 2; computationally less demanding than transition state calculations) may serve as a useful qualitative indicator of overall intramolecular directing group selectivity, assuming similar *ortho*-C–H activation kinetic barriers for reaction at either directing group.[24] However, we also recognised that computational predictions and observed selectivities reported in our earlier work may have been biased – in favour of sulfonamide selectivity – by both the steric encumbrance and electron-withdrawing power of the trifluoromethyl (CF_3) substituent in drug series **1** (Scheme 1).[24] Specifically, the CF_3 group directly attenuates the binding ability of the competing pyrazole directing group. However, the CF_3 group only indirectly influences the remote sulfonamide in the same molecule. The CF_3 group may, then, exaggerate the observed sulfonamide over pyrazole directing group chemoselectivity differences between catalysts **2a** and **2b** (Scheme 1). Indeed, calculation of Sterimol[41] (steric) and NBO[42] charge (electronic) differences in methoxy analogues of **1**, **4a** (CF_3 pyrazole substituent) and **4b** (CF_2H pyrazole substituent), supports this view (Scheme 3).

The CF_3 group is calculated to be distinctly larger (in two dimensions) than CF_2H in the analogous molecule. Not surprisingly, CF_3 also withdraws more electron density from the Lewis basic pyrazole nitrogen relative to the CF_2H analogue.

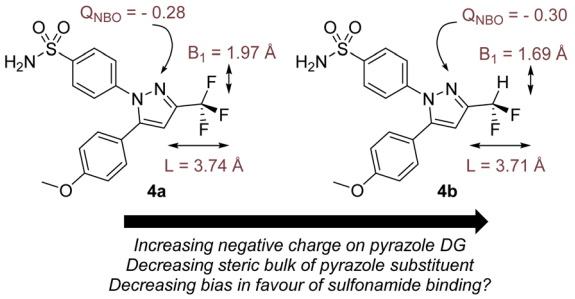

Scheme 3 Calculated differences in CF_3 *versus* CF_2H for substrates **4a** and **4b**, respectively. The pyrazole in substrate **4b** is more basic and less sterically encumbered than the pyrazole in **4a**, making it potentially more competitive with the sulfonamide directing group for catalyst binding.

Using qualitative binding free energy calculations to explore product-determining directing group chemoselectivity and sulfonamide-selective catalyst design

With the aforementioned observations in mind, we aimed initially to answer two key questions in the current study: (i) can intramolecular directing group selectivity be more generally (within the realms of Ir-catalysed C–H activation) predicted *via* qualitative $\Delta(\Delta G_{bind})$ calculations alone, and (ii) to what extent do electronic and steric effects in the competing pyrazole directing group (*i.e.* CF_3 derivative **4a** *vs.* CF_2H derivative **4b**) influence sulfonamide binding when employing less encumbered catalyst **2a**? Furthermore, in the course of these investigations, we also established the deuterium labelling profiles with further derivatives of drug series **1**, and evaluated the broader ability of binding free energy calculations to qualitatively guide rational catalyst design for enhanced sulfonamide-selective C–H deuteration.

Our hypothesis on the combined influences of catalyst and substrate structure on directing group chemoselectivity is shown in Scheme 4. For the smaller catalyst **2a**, we showed previously that sulfonamide selectivity was consistent with the binding model that harnesses secondary hydrogen bonding between the chloride ligand and the sulfonamide directing group (Scheme 4, top left).[24] It was theorised that this preference would switch to pyrazole binding upon a switch of CF_3 for CF_2H substitution (Scheme 4, top right). Conversely, the more rigid and sterically encumbered ligand sphere in catalyst **2b** is more discerning between these directing groups on the basis of directing group size. The planar pyrazole binds preferentially over the larger tetrahedral sulfonamide, regardless of CF_3 or CF_2H substitution on the pyrazole ring (Scheme 4, bottom). Indeed, catalyst **2b** is unable to efficiently label even simple aryl 1° sulfonamides.[24] Based on all of this, the switchable directing group chemoselectivity is predicted to be unique to NHC/Cl precatalyst **2a** (*cf.* **2b**).

Building on our initial hypothesis, our investigations towards catalysts of enhanced effectiveness for sulfonamide-directed C–H activation and labelling began by assessing the relative binding energies of drug derivatives **4a** and **4b** to the activated Ir(III) dideuteride forms of Ir(I) precatalysts **2a** and **2b** (Scheme 5). For bulky catalyst **2b**, pyrazole binding was

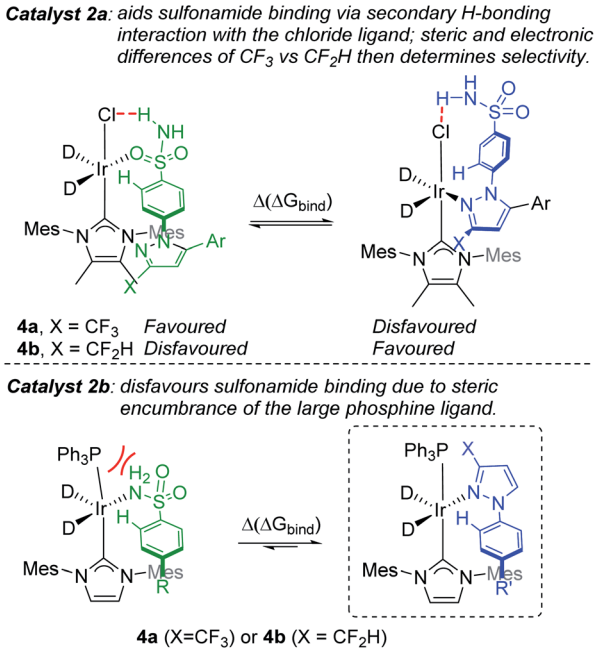

Scheme 4 Hypothesised binding modes for sulfonamide and pyrazole directing groups.

predicted to dominate in both drug derivatives, **4a** (CF_3) and **4b** (CF_2H); Scheme 5 (bottom). In the case of smaller catalyst **2a**, however, the sulfonamide and pyrazole directing group binding energies were relatively balanced, with sulfonamide binding favoured in CF_3 derivative **4a**, but pyrazole binding dominating in CF_2H derivative **4b**; Scheme 5 (top).

Encouragingly, consideration of the sulfonamide and pyrazole binding energies was sufficient to qualitatively understand and predict the experimentally observed labelling, and thus directing group chemoselectivity (in binary terms), in all cases (Scheme 5). Remarkably, it appeared that qualitative binding free energy calculations were able to capture directing

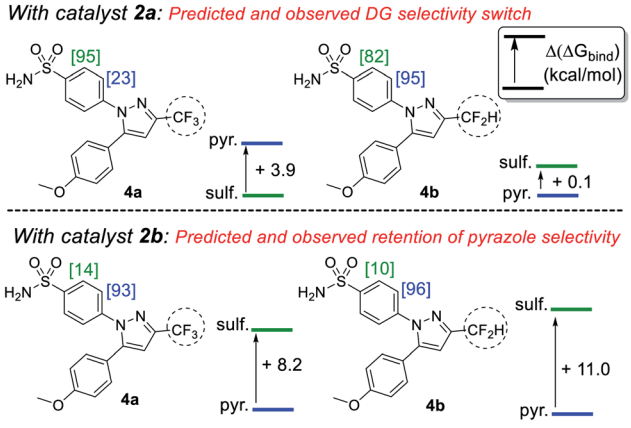

Scheme 5 Experimental directing group chemoselectivity in Ir-catalysed deuteration *versus* qualitative DFT binding free energy differences for sulfonamide (sulf.) and pyrazole (pyr.) directing groups. [X] = %*D* incorporation based on triplicate runs. Conditions: substrate (0.05 mmol), catalyst (6.5 mol%), D_2 (1 atm), DCM, 25 °C, 2 h.

group selectivity switching (Scheme 5, top) and selectivity retention (Scheme 5, bottom) for each combination of substrate and catalyst. This comparison of theoretical directing group binding energies $\Delta(\Delta G_{bind})$ *versus* experimentally observed deuterium labelling selectivity highlighted the apparent qualitative and predictive use of these simple calculations in discriminating intramolecular directing groups (Scheme 5). This was consistent with a number of previous observations emerging from our own laboratories,[18,22,24,25,39] as well as those reported by Derdau and co-workers.[13] As a result, these observations presented an opportunity to redesign catalyst **2a** in an attempt to reinstate high sulfonamide directing group chemoselectivity in CF_2H derivative **4b**, even in the face of the intrinsically favoured competitor pyrazole directing group present in the same substrate.

Redesigning catalyst 2a towards improved sulfonamide selectivity

From our previous studies with catalysts such as **2a**, alteration of the NHC ligand size had the most marked impact on catalyst activity across the various design parameters considered.[24] Accordingly, percent buried volume ($\%V_{bur}$) calculations[43–45] suggested that new catalysts **2c**, [(COD)Ir(IPr^{Me})(Cl)], and **2d**, [(COD)Ir(IPent)(Cl)], progressively more sterically encumbered analogues of **2a** (Scheme 6), would provide a steric clash with the CF_2H substituent that would diminish deuterium labelling *via* the pyrazole unit.

Indeed, on comparing $\Delta(\Delta G_{bind})$ and experimentally observed deuterium labelling selectivities in substrate **4b** with catalysts **2a**, **2c**, and **2d**, sulfonamide selectivity was restored with progressive efficacy using larger catalysts **2c** then **2d** (Scheme 7). Table 1 (*vide infra*) reveals the broader effectiveness, synthetic utility, and limits of redesigned catalyst **2d** (the most encumbered in the series), demonstrating previously unattainable chemoselectivity for the sulfonamide directing group in the face of the competing pyrazole.

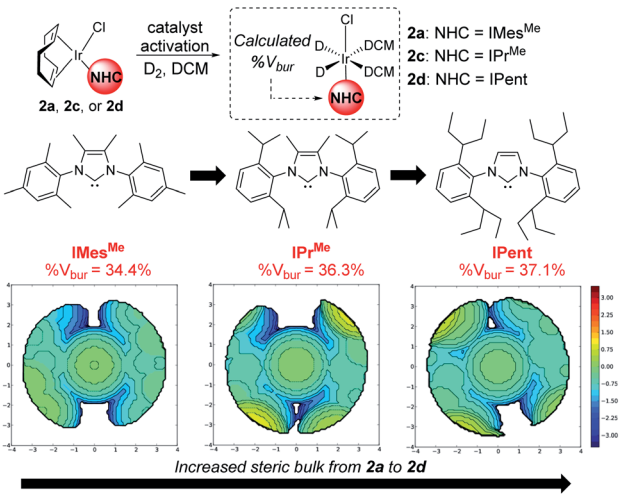

Scheme 6 Redesign of precatalyst **2a** to **2d** *via* consideration of NHC sterics.

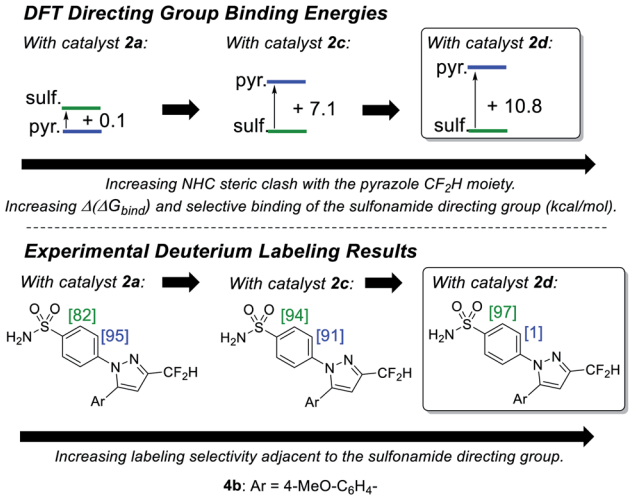

Scheme 7 Qualitative correlation between increased sulfonamide binding preference and improved labelling selectivity for substrate **4b**. [X] = *%D* incorporation based on triplicate runs. Conditions: substrate (0.05 mmol), catalyst (6.5 mol%), D_2 (1 atm), DCM, 25 °C, 2 h. Level of theory: M06/6-31G*/Stuttgart BS + ECP (Ir).

Table 1 3rd Generation sulfonamide-labelling catalyst for optimal selectivity against intrinsically favoured pyrazole

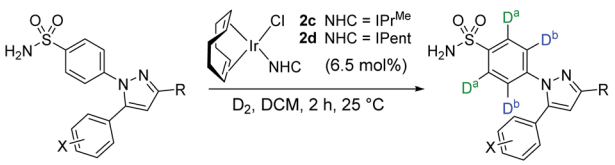

Entry	Catalyst	Substrate	R	X	$\%D_a$ (sulf.)	$\%D_b$ (pyr.)
1	**2c**	**4b**	CF_2H	4-MeO	94	91
2	**2d**	**4b**	CF_2H	4-MeO	97	1
3	**2c**	**4c**	CF_2H	4-F	96	31
4	**2d**	**4c**	CF_2H	4-F	97	2
5	**2c**	**4d**	CF_2H	3-F, 4-MeO	95	15
6	**2d**	**4d**	CF_2H	3-F, 4-MeO	95	1
7	**2c**	**4e**	Me	4-Me	87	25
8	**2d**	**4e**	Me	4-Me	81	13
9	**2c**	**4f**	H	4-Me	26	94
10	**2d**	**4f**	H	4-Me	24	96

Kinetic analysis of intramolecular directing group chemoselectivity across the evolving catalyst series

Importantly, the vastly improved sulfonamide directing group chemoselectivity with catalyst **2d** *versus* catalyst **2a** is consistent with differences in the temporal profiles of deuterium labelling *ortho* to each directing group in substrate **4b** using catalysts **2a**, **2c**, and **2d** in the series (Scheme 8). More specifically, kinetic profiling showed that there were modest relative rate differences in labelling next to the sulfonamide *versus* pyrazole directing groups when catalyst **2a** or **2c** was used (Scheme 8, left and middle panels). However, with catalyst **2d**, the C–H positions *ortho* to the sulfonamide in **4b** were labelled over 400

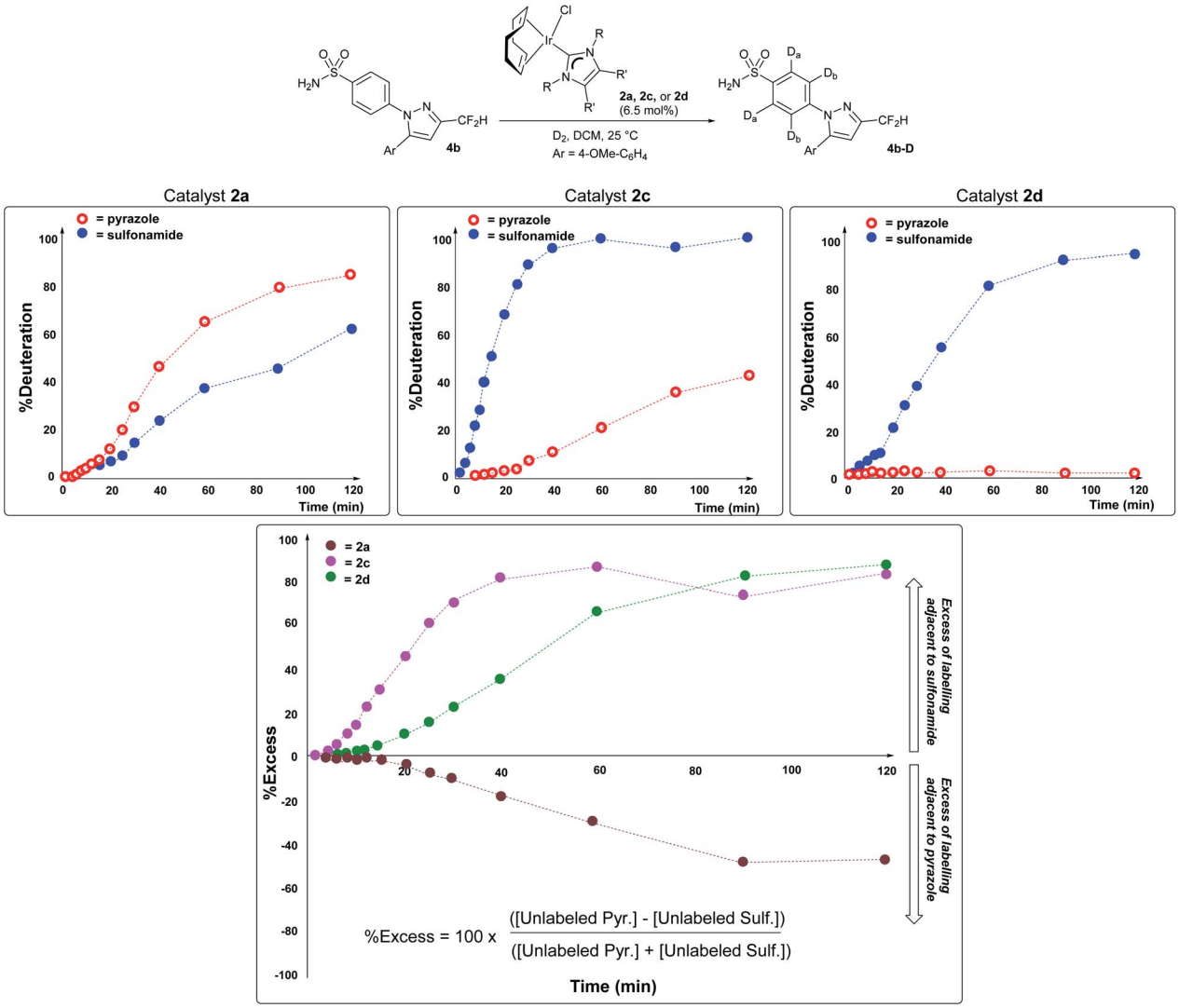

Scheme 8 Top row, left to right: time course plots evidencing increased kinetic selectivity for labelling adjacent to the sulfonamide over the pyrazole directing group as the catalyst becomes more sterically encumbered. The visible induction period in each time course reflects the precatalyst Ir(I) → Ir(III) activation process, a simplified representation of which is shown at the top of Scheme 6. Bottom panel: dynamic selectivity for labelling adjacent to the sulfonamide directing group over the pyrazole as a function of time, expressed as a percentage excess, with the positive *y*-values denoting a preference for sulfonamide over pyrazole. Each series of points and dashed lines represents a different catalyst employed.

times faster than those C–H positions adjacent to the pyrazole (Scheme 8, rightmost panel). Catalyst **2d** was also the only catalyst in the series to enable high levels of sulfonamide selectivity to be maintained throughout the entire time period in which the profile was monitored (Scheme 8, right). This selectivity differs from that of catalyst **2c**, where selectivity for sulfonamide over pyrazole labelling was eroded over the monitored time course. Finally, it should be noted that the kinetic results qualitatively agree with the single-point deuteration results reported for reactions with **4b** (Scheme 7).[46] The direction of selectivity remains the same across all cases in Schemes 7 and 8, and differences in absolute %*D* are likely due to the different scale and vessel shape required to capture the kinetic information reported in Scheme 8.[53]

Probing the possible non-innocence of a distal directing group in a bifunctional substrate

In the IPr^{Me}[47] or IPent[48] ligands of 2nd and 3rd generation pre-catalysts **2c** and **2d**, respectively, the enhanced steric interaction with the CF_2H group on the pyrazole of substrate **4b** appeared to be manifested in $\Delta(\Delta G_{bind})$, and is exemplified in the resultant DFT-calculated structures for the interaction of **4b** and **2d** (Scheme 9). Crucially, when the pyrazole of **4b** is bound to the iridium centre (Scheme 9, right), our standard and precedented gas phase calculation protocol suggested that the distal sulfonamide is not innocent. Whilst the pyrazole binds to the metal centre, the gas phase calculation shows the sulfonamide binding *via* a NH–Cl hydrogen bond, resulting in an unfavourable distortion of the bound substrate. This apparent

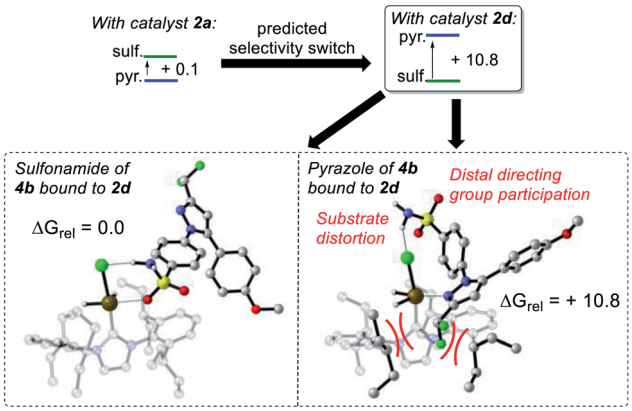

Scheme 9 Gas-phased calculated directing group switch on using catalyst **2d**, where the sulfonamide binds in preference to the pyrazole due, in part, to coupled directing group behaviour. Level of theory: M06/6-31G* (Gas)/Stuttgart BS + ECP (Ir).

distortion is in addition to the steric clash between the CF_2H substituent and the NHC ligand. Using the $\Delta(\Delta G_{bind})$ method and our standard level of theory in DFT calculations, the secondary interaction of the distal sulfonamide would appear to suggest that directing groups within the same molecule cannot be assumed to be acting independently of one another (Scheme 9, right).[24] In this case, and despite their apparent spatial separation, intramolecular directing group reactivity could be considered coupled, and thus suggest that secondary interactions emerging from the binding event can influence a given directing group binding mode. Note that no such secondary interaction is apparent from gas phase calculations that have the sulfonamide participating as the main directing group bound directly to the metal (Scheme 9, left).

It is important to note that the evolution towards catalyst **2d** was considered in concert with maintaining the chloride as a partner ligand. Indeed, the employment of IPent in **2d** is rendered obsolete if the chloride is replaced with a weakly-coordinating MeCN ligand (Scheme 10). Accordingly, the result of chloride abstraction is to reverse the directing group chemoselectivity back to the pyrazole. This result might be interpreted as removing the key additional interaction in substrate binding apparent in the DFT calculations (Scheme 9, right). The result in Scheme 10 may alternatively be interpreted as a change in catalyst speciation facilitated by the abstraction of chloride.

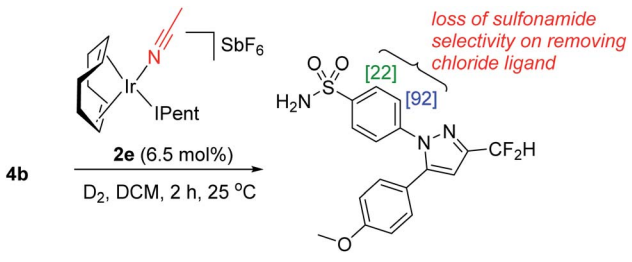

Scheme 10 Replacing the chloride ligand in **2d** with weakly bound acetonitrile in **2e** destroys the ligand synergy that produces sulfonamide directing group chemoselectivity. [X] = %*D* incorporation based on triplicate runs.

Up to this point in the investigation, all experimental observations supported the initial hypothesis in which simple $\Delta(\Delta G_{bind})$ calculations could be used as a qualitative predictor of intramolecular directing group chemoselectivity, and thus serve as a guiding tool for enhanced sulfonamide-selective catalyst design. To test the generality of the DFT-guided catalyst design strategy, catalysts **2c** and **2d** were applied to the labelling of 4 additional celecoxib derivatives (Table 1). Consistent with results first noted in Scheme 7, complex **2d** was shown to provide good to excellent sulfonamide selectivity for 3 of the 4 additional substrates (entries 4, 6, and 8). Only when substitution was removed from the pyrazole (R = H, entries 9 and 10) was it shown that catalyst **2d** was unable to maintain sulfonamide selectivity. Overall, these results appeared to demonstrate the power of rational catalyst design in overcoming intrinsic directing group chemoselectivity (Scheme 1). As well as enhancing our understanding of site-selective C–H activation, this ability to control deuterium incorporation and isotope distribution in a medicinal candidate represents a key resource for metabolic studies in early-stage drug design.[49,50]

Deconstructing binding energies to probe the structural origins of improved sulfonamide directing group chemoselectivity with catalysts 2c and 2d

Having demonstrated the qualitative *a priori* catalyst design strategy with $\Delta(\Delta G_{bind})$, the underlying cause of differences in directing group binding free energies was investigated. Any difference in the directing group binding electronic energies (E_{bind}) represents the combined impact of favourable substrate–catalyst interactions (E_{int}) and unfavourable structural distortions (E_{dist}), as in eqn (1):

$$E_{bind} = E_{int} + E_{dist} \quad (1)$$

Values E_{int} and E_{dist} were derived by employing the Boys–Bernardi counterpoise scheme, which calculates electronic energies of catalyst and substrate fragments from previously optimised geometries.[3,51,52] As detailed in Scheme 11, deconstructed directing group binding electronic energies for CF_2H-containing substrate **4b** were assessed. Consistent with the $\Delta(\Delta G_{bind})$ free energy calculations, moving from catalyst **2a** to **2d** progressively improves the overall binding electronic energy for the sulfonamide over the competing pyrazole (E_{bind}; blue). In addition, however, elucidation of E_{dist} and E_{int} for each binding event revealed that improved sulfonamide selectivity with catalysts **2c** and **2d** appears to be driven by lowered levels of structural distortion (E_{dist}; red) rather than enhanced favourable interactions (E_{int}; green). Indeed, the distortion caused by binding the pyrazole directing group overrides intrinsically-favourable interaction energies that would otherwise suggest preference for the pyrazole *versus* the sulfonamide. This is consistent with the apparent substrate distortion features discussed earlier for the gas-phase calculated structures used to probe $\Delta(\Delta G_{bind})$ for catalyst **2d** and substrate **4b** (Scheme 9, right).

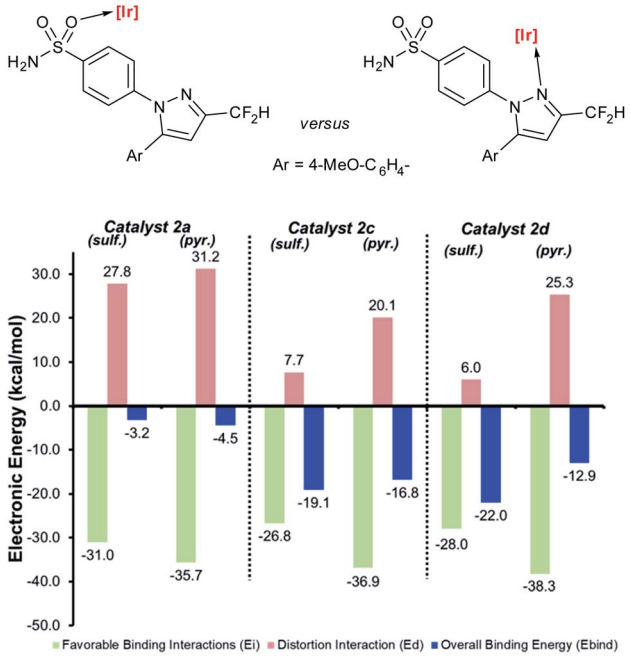

Scheme 11 Deconstructed directing group binding electronic energies for substrate **4b** to catalysts **2a**, **2c**, and **2d**. Progression towards catalyst **2d** serves to minimise substrate distortion when the sulfonamide is bound and maximise distortion when the pyrazole is bound. The more negative the blue number, the more favoured the binding of that directing group. Level of theory: M06/6-31G*/Stuttgart BS + ECP (Ir).

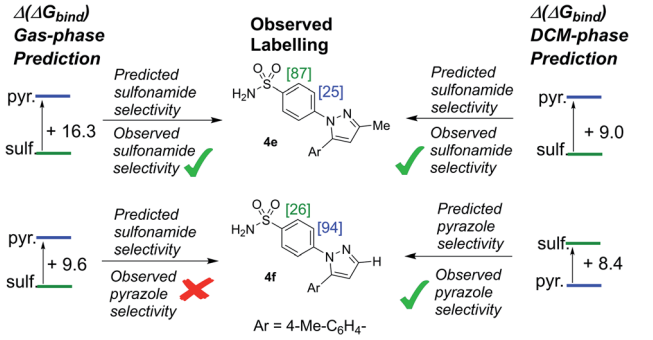

Scheme 12 The limiting case for sulfonamide selective labelling with catalyst **2c** also presents the limiting case for prediction of intramolecular directing group chemoselectivity *via* the gas-phase $\Delta(\Delta G_{bind})$ catalyst design parameter (left-hand side). Only with structure re-optimisation in DCM was the predictive power of $\Delta(\Delta G_{bind})$ fully re-established. [X] = experimental *%D* incorporation based on duplicate or triplicate runs. Conditions: substrate (0.05 mmol), catalyst (6.5 mol%), D_2 (1 atm), DCM, 25 °C, 2 h. Level of theory: M06/6-31G*/Stuttgart basis set + ECP (Ir). Left-side: gas-phase; right-side: DCM solvent model included.

Limitations of the $\Delta(\Delta G_{bind})$ catalyst design strategy

To this stage, our attempts to design a catalyst for enhanced sulfonamide directing group chemoselectivity had been met with a somewhat compelling and consistent design strategy in both $\Delta(\Delta G_{bind})$ and deconstructed electronic energies *via* the counterpoise method. However, having found the experimental limit in which bulky catalysts **2c** and **2d** fails to deliver sulfonamide selective deuterium labelling (Table 1, entry 10, substrate **4f**), it was important to revisit $\Delta(\Delta G_{bind})$ to probe whether the method was able to predict the switch back to pyrazole selectivity on moving to the unsubstituted pyrazole-containing substrate **4f**. Interestingly, our original $\Delta(\Delta G_{bind})$ method and chosen level of theory failed to account for the observed switch back to pyrazole selectivity for substrate **4f** and catalyst **2c** (used as the less computationally demanding variant of catalyst **2d**; Scheme 12).

When the breakdown of the $\Delta(\Delta G_{bind})$ method was investigated further, it was found that inclusion of a DCM continuum solvation model in the binding energy calculations caused crucial structural changes that switched the calculated order of directing group binding strength for substrate **4f**. Specifically, in the pyrazole bound state, the supposed secondary interaction of the sulfonamide with the chloride ligand *via* the hydrogen bond NH–Cl, found in the earlier gas phase calculation, was lost in the re-optimised DCM-solvated structure (Scheme 13). This, in turn, had the knock-on effect of reducing the substrate distortion for the pyrazole bound conformer. Ultimately, inclusion of DCM solvation in geometry optimisations and thermal calculations corrected the $\Delta(\Delta G_{bind})$ prediction, but served as an illustrative case of where gas-phase binding energy calculations as descriptors of intramolecular directing group chemoselectivity can break down.

Perhaps more strikingly, when the DCM-solvated structures from Scheme 13 were investigated *via* the counterpoise electronic energy decomposition method (Scheme 14), the predicted binding electronic energies did not match the revised $\Delta(\Delta G_{bind})$ values from DCM re-optimisation, and therefore did not match the experimental outcome. It is worth re-emphasising that the counterpoise method is one that requires single point gas-phase structures, even if those structures were found using solvated optimisation methods.

For methyl-substituted substrate **4e**, rigorous (Boys–Bernardi) binding energies calculated from both gas-phase and DCM-solvated structures matched the experimental directing group chemoselectivity; both gas-phase and DCM-solvated methods predicted majority deuterium labelling adjacent to the sulfonamide directing group (see ESI†). However, for unsubstituted pyrazole substrate **4f**, using either gas-phase or DCM-

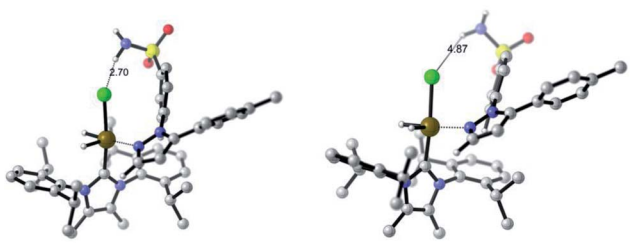

Scheme 13 Comparison of substrate **4f** binding conformation on catalyst **2c**. Left: gas-phase; right: with DCM solvation model applied. The latter decreases the emphasis of the secondary H-bond from the sulfonamide to the chloride ligand and alleviates substrate distortion.

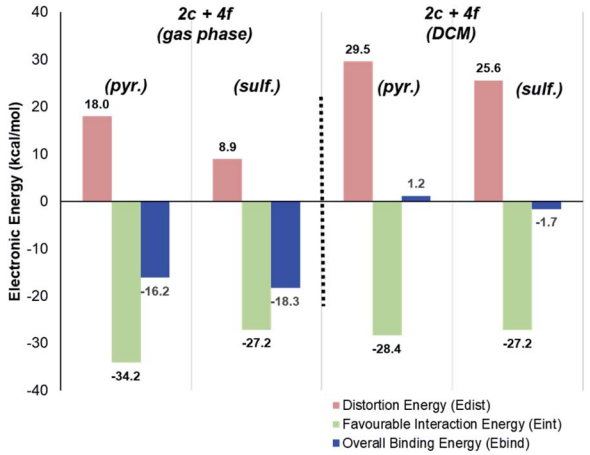

Scheme 14 Deconstructed directing group binding energies for catalyst **2c** and substrate **4f**, as calculated in the gas phase and DCM-solvated structures. In both calculation regimes, the sulfonamide directing group is wrongly predicted to be the favoured directing group.

solvated structures, were unable to predict the experimental outcome *via* the counterpoise method (Scheme 14). Only when free energies were considered, inclusive of all thermal corrections to electronic energies, were the binding energy differences between sulfonamide and pyrazole in full agreement with observed *ortho*-labelling outcomes (Scheme 12).

Conclusions

In conclusion, this case study has shown the use and limitations of directing group binding energy calculations to guide the development of new iridium-based complexes which deliver enhanced chemoselectivity in the C–H activation and deuteration of 1° aryl sulfonamides in the face of a competing directing group. Additionally, these endeavours have revealed several important findings of immediate relevance to the broader C–H activation community:

1. For substrates bearing two directing groups, ground state (thermodynamic) $\Delta(\Delta G_{bind})$ calculations can serve as a simple, qualitative measure for directing group chemoselectivity, without requirement for detailed transition state calculations, so long as the use or absence of solvation is carefully considered.

2. The inclusion of solvation in $\Delta(\Delta G_{bind})$ calculations can lead to notable inconsistencies in conclusions drawn from more detailed binding energy deconstructions, as facilitated by, for example, the counterpoise method.

In sum, the identification of catalyst **2d** has the potential to deliver direct applications in the isotopic labeling community. Further, we also believe that the mechanistic findings of this study will be of interest as part of emerging late-stage C–H functionalisation strategies as applied to densely functionalised molecules. The consequences of these outputs on labelling and C–H functionalisation are the subjects of further investigation in our laboratories.

Abbreviations

COD	Cyclooctadiene
DFT	Density functional theory
DG	Directing group
HIE	Hydrogen isotope exchange
IPent	1,3-bis(2,6-di(pentan-3-yl)phenyl)imidazol-2-ylidene)
IPr^{Me}	1,3-bis(2,6-di-*iso*-propylphenyl)-4,5-dimethylimidazol-2-ylidene
Mes	Mesityl
NHC	*N*-Heterocyclic carbene
NBO	Natural Bond Orbital

Author contributions

WJK – conceptualization, funding acquisition, project administration, resources, supervision, writing – review & editing. GJK – data curation, investigation, visualization. MR – conceptualization, data curation, formal analysis, funding acquisition, investigation, methodology, visualization, writing – original draft, writing – reviewing & editing. TT – project administration, resources, supervision, validation.

Conflicts of interest

There are no conflicts to declare.

Acknowledgements

The authors would like to thank the Carnegie Trust for the Universities of Scotland and the Leverhulme Trust for funding (M. R.), and the EPSRC UK National Mass Spectrometry Facility at Swansea University for analyses.

Notes and references

1 G.-J. Cheng, X. Zhang, L. W. Chung, L. Xu and Y.-D. Wu, *J. Am. Chem. Soc.*, 2015, **137**, 1706–1725.
2 G. Jindal, H. K. Kisan and R. B. Sunoj, *ACS Catal.*, 2015, **5**, 480–503.
3 I. Fernández and F. M. Bickelhaupt, *Chem. Soc. Rev.*, 2014, **43**, 4953–4967.
4 A. S.-K. Tsang, I. A. Sanhueza and F. Schoenebeck, *Chem. Eur. J.*, 2014, **20**, 16432–16441.
5 J. Jover and N. Fey, *Chem.–Asian J.*, 2014, **9**, 1714–1723.
6 A. G. Maldonado and G. Rothenberg, *Chem. Soc. Rev.*, 2010, **39**, 1891–1902.
7 K. N. Houk and P. H.-Y. Cheong, *Nature*, 2008, **455**, 309–313.
8 D. Balcells, E. Clot and O. Eisenstein, *Chem. Rev.*, 2010, **110**, 749–823.
9 H. M. L. Davies and D. Morton, *J. Org. Chem.*, 2016, **81**, 343–350.
10 T. Cernak, K. D. Dykstra, S. Tyagarajan, P. Vachal and S. W. Krska, *Chem. Soc. Rev.*, 2016, **45**, 546–576.

11 J. Yamaguchi, A. D. Yamaguchi and K. Itami, *Angew. Chem., Int. Ed.*, 2012, **51**, 8960–9009.
12 L. McMurray, F. O'Hara and M. J. Gaunt, *Chem. Soc. Rev.*, 2011, **40**, 1885–1898.
13 M. Valero, T. Kruissink, J. Blass, R. Weck, S. Güssregen, A. T. Plowright and V. Derdau, *Angew. Chem., Int. Ed.*, 2020, **59**, 5626–5631.
14 Y. Dong, X. Zhang, J. Chen, W. Zou, S. Lin and H. Xu, *Chem. Sci.*, 2019, **10**, 8744–8751.
15 G. B. Boursalian, W. S. Ham, A. R. Mazzotti and T. Ritter, *Nat. Chem.*, 2016, **8**, 810–815.
16 J. M. Curto and M. C. Kozlowski, *J. Am. Chem. Soc.*, 2015, **137**, 18–21.
17 S. R. Neufeldt, G. Jiménez-Osés, J. R. Huckins, O. R. Thiel and K. N. Houk, *J. Am. Chem. Soc.*, 2015, **137**, 9843–9854.
18 J. Devlin, W. Kerr, D. Lindsay, T. McCabe, M. Reid and T. Tuttle, *Molecules*, 2015, **20**, 11676–11698.
19 A. G. Green, P. Liu, C. A. Merlic and K. N. Houk, *J. Am. Chem. Soc.*, 2014, **136**, 4575–4583.
20 Y. Ma, J. Liang, D. Zhao, Y. Chen, J. Shen and B. Xiong, *RSC Adv.*, 2014, **4**, 17262–17264.
21 W. M. C. Sameera, S. Maeda and K. Morokuma, *Acc. Chem. Res.*, 2016, **49**, 763–773.
22 W. J. Kerr, G. J. Knox, M. Reid, T. Tuttle, J. Bergare and R. A. Bragg, *ACS Catal.*, 2020, **10**, 11120–11126.
23 W. J. Kerr, M. Reid and T. Tuttle, *Angew. Chem., Int. Ed.*, 2017, **56**, 7808–7812.
24 W. J. Kerr, M. Reid and T. Tuttle, *ACS Catal.*, 2015, **5**, 402–410.
25 J. A. Brown, A. R. Cochrane, S. Irvine, W. J. Kerr, B. Mondal, J. A. Parkinson, L. C. Paterson, M. Reid, T. Tuttle, S. Andersson and G. N. Nilsson, *Adv. Synth. Catal.*, 2014, **356**, 3551–3562.
26 M. Reid, in *Topics in Organometallic Chemistry*, Springer Berlin Heidelberg, Berlin, Heidelberg, 2020, pp. 1–32.
27 J. Atzrodt, V. Derdau, W. J. Kerr and M. Reid, *Angew. Chem., Int. Ed.*, 2018, **57**, 3022–3047.
28 W. J. S. Lockley, A. McEwen and R. Cooke, *J. Labelled Compd. Radiopharm.*, 2012, **55**, 235–257.
29 P. H. Allen, M. J. Hickey, L. P. Kingston and D. J. Wilkinson, *J. Labelled Compd. Radiopharm.*, 2010, **53**, 731–738.
30 G. N. Nilsson and W. J. Kerr, *J. Labelled Compd. Radiopharm.*, 2010, **53**, 662–667.
31 R. Salter, *J. Labelled Compd. Radiopharm.*, 2010, **53**, 645–657.
32 M. Parmentier, T. Hartung, A. Pfaltz and D. Muri, *Chem.–Eur. J.*, 2014, **20**, 11496–11504.
33 M. C. Lehman, J. B. Gary, P. D. Boyle, M. S. Sanford and E. A. Ison, *ACS Catal.*, 2013, **3**, 2304–2310.
34 J. Zhou and J. F. Hartwig, *Angew. Chem., Int. Ed.*, 2008, **47**, 5783–5787.
35 C. A. Swift and S. Gronert, *Angew. Chem., Int. Ed.*, 2015, **54**, 6475–6478.
36 J. L. Rhinehart, K. A. Manbeck, S. K. Buzak, G. M. Lippa, W. W. Brennessel, K. I. Goldberg and W. D. Jones, *Organometallics*, 2012, **31**, 1943–1952.
37 V. M. Iluc, A. Fedorov and R. H. Grubbs, *Organometallics*, 2012, **31**, 39–41.
38 C. M. Yung, M. B. Skaddan and R. G. Bergman, *J. Am. Chem. Soc.*, 2004, **126**, 13033–13043.
39 W. J. Kerr, D. M. Lindsay, P. K. Owens, M. Reid, T. Tuttle and S. Campos, *ACS Catal.*, 2017, **7**, 7182–7186.
40 J. Tomasi, B. Mennucci and R. Cammi, *Chem. Rev.*, 2005, **105**, 2999–3093.
41 K. C. Harper, E. N. Bess and M. S. Sigman, *Nat. Chem.*, 2012, **4**, 366–374.
42 A. E. Reed, R. B. Weinstock and F. Weinhold, *J. Chem. Phys.*, 1985, **83**, 735–746.
43 L. Falivene, Z. Cao, A. Petta, L. Serra, A. Poater, R. Oliva, V. Scarano and L. Cavallo, *Nat. Chem.*, 2019, **11**, 872–879.
44 H. Clavier and S. P. Nolan, *Chem. Commun.*, 2010, **46**, 841–861.
45 A. Poater, B. Cosenza, A. Correa, S. Giudice, F. Ragone, V. Scarano and L. Cavallo, *Eur. J. Inorg. Chem.*, 2009, **2009**, 1759–1766.
46 The necessary change in glassware to facilitate kinetic experiments (versus single point experiments) is presumed to modify the surface area and overall concentration of deuterium gas present in the system relative to substrate concentration.
47 S. Gaillard, X. Bantreil, A. M. Z. Slawin and S. P. Nolan, *Dalton Trans.*, 2009, 6967.
48 M. Pompeo, R. D. J. Froese, N. Hadei and M. G. Organ, *Angew. Chem., Int. Ed.*, 2012, **51**, 11354–11357.
49 J. Atzrodt, V. Derdau, W. J. Kerr and M. Reid, *Angew. Chem., Int. Ed.*, 2018, **57**, 1758–1784.
50 J. Atzrodt and V. Derdau, *J. Labelled Compd. Radiopharm.*, 2010, **53**, 674–685.
51 K. N. Kirschner, J. B. Sorensen and J. P. Bowen, *J. Chem. Educ.*, 2007, **84**, 1225.
52 S. F. Boys and F. Bernardi, *Mol. Phys.*, 1970, **19**, 553–566.
53 J. Luo, Y. Wu, H. S. Zijlstra, D. A. Harrington and J. S. McIndoe, Mass transfer and convection effects in small-scale catalytic hydrogenation, *Catal. Sci. Technol.*, 2017, **7**, 2609–2615.